to a lack of magnetic homogeneity in these samples with the possible formation of rhodium–rhodium clusters. The paramagnetic data further supports the possibility of formation of rhodium–rhodium clusters at large rhodium concentrations.

Acknowledgment. The authors with to thank the Exxon Research and Engineering Co., Linden, NJ, for the support of J.C. Acknowledgment is also made to the National Science Foundation, Washington, D.C. (Grant No. DMR79-23605), for the support of K.D. and to the Materials Research Laboratory Program at Brown University for the use of its facilities.

Registry No. CoS_2, 12013-10-4; RhS_2, 12038-73-2; $(NH_4)_3RhCl_6$, 15336-18-2; $[Co(NH_3)_5Cl]Cl_2$, 13859-51-3.

Contribution from Ames Laboratory—DOE[1] and Department of Chemistry, Iowa State University, Ames, Iowa 50011

A Second Infinite-Chain Form of Zirconium Diiodide (β) and Its Coherent Intergrowth with α-Zirconium Diiodide

JOHN D. CORBETT* and DENNIS H. GUTHRIE

Received August 26, 1981

Syntheses of the previously reported monoclinic (α) ZrI_2 contain a second orthorhombic (β) phase which is isostructural with WTe_2, space group $Pmn2_1$ (No. 31) with a = 3.7442 (5) Å, b = 6.831 (1) Å, and c = 14.886 (2) Å and Z = 4. Refinement with 768 unique reflections measured on an automatic diffractometer with monochromatic Mo Kα radiation gave R = 0.051 and R_w = 0.070. β-ZrI_2 contains sheets in which infinite zigzag chains of zirconium (d_{Zr-Zr} = 3.185 (3) Å) lie between puckered iodine layers. The structure is very similar to that reported for α-ZrI_2 and differs principally in shear displacements of adjacent layers. The two phases evidently always intergrow with one another in various proportions, a property which accounts for apparent "superlattice" reflections and for a powder pattern of the "phase" which is much more complex than expected. Both structures may be derived from that in the lattice-equivalent supergroup *Pmnb* (No. 62) by shear displacements of the layers in second-order phase transitions. A residual electron density which apparently originates in the intergrowth or defect regions of the β-ZrI_2 crystals may imply a substoichiometry, in support of bulk analyses of Zr:I $\simeq$ 1.05:2.

Introduction

Among the zirconium halides with oxidation states below +3 only the cluster phases Zr_6X_{12} are common to chloride, bromide, and iodide;[2-4] otherwise the iodides appear to be quite distinctive. A polymorph of the cluster diiodide Zr_6I_{12} has recently been reported in monoclinic α-ZrI_2 which as the layered β-$MoTe_2$ structure.[5] This may be described as a distortion of a CdI_2-like arrangement in which zirconium atoms have been systematically displaced from the centers of octahedral (trigonal antiprismatic) interstices so as to form infinite zigzag chains of strongly bonded metal atoms (d = 3.182 Å) between pairs of iodine layers. A comparable phase has not been found with chloride and bromide; rather these form a sheet structure with $ZrCl_2$ (3R-MoS_2-type), substoichiometric superstructures for $Zr_{1+x}Cl_2$, and a probably related bromide.[6] In addition both the chloride and bromide form a double-metal-layered monohalide with close-packed sheets sequenced X–Zr–Zr–X.[7,8] The equivalent iodide phase has not yet been obtained in spite of extensive investigation.

Continuing studies of the lower iodides have been plagued by a number of complications encountered with the diiodide, namely, (1) Guinier powder patterns for "α-ZrI_2" which are inevitably much more complex than that calculated for the known structure, even for patterns taken of ground "single" crystals, (2) evidence of possible superstructure reflections in Weissenberg photographs of α-ZrI_2, and (3) some analytical evidence for substoichiometry (I:Zr $\approx$ 1.90 $\pm$ 0.05:1) in polycrystalline samples,[9] although no indication of this was found in the reported α-ZrI_2 structure. Most of these problems have now been clarified with the identification of a second orthorhombic form of the layered ZrI_2 structure (β) which shows extensive intergrowth with the monoclinic α form.

Experimental Section

The methods of handling these materials and the synthetic techniques utilized have already been described.[5] Crystals from which the structure of α-ZrI_2 was solved were formed from long-term reactions of ZrI_4 with a large excess of Zr in welded tantalum containers at ca. 750–850 °C which were then cooled by turning off the power to the furnace. Black, lath- to blade-shaped crystals which exhibit a gold reflectance form, presumably via a transport reaction which involves a ZrI_3(g) intermediate. Occasionally crystals were found in earlier studies which were apparently orthorhombic either from indexing on the automatic diffractometer or according to Weissenberg photographs or from both, and these exhibited unit cell axes closely resembling those of the monoclinic α (where β = 95.7°).

Diffraction data were collected on three different orthorhombic crystals, two of which came from high-temperature reactions at 900–950 °C and gave broad peaks and considerable streaking. The structure of these two, though evidently basically the same as reported herein, would not define below $R \approx 0.20$ because of apparent disorder. A much more suitable crystal came from a relatively low-temperature reaction of a 44:1 mole ratio of Zr strips and ZrI_4 for about 8 weeks at 770 °C. A rectangular prism ~0.74 × 0.081 × 0.056 mm was sealed into a 0.2-mm diameter capillary within the drybox and examined by oscillation and Weissenberg photographic techniques. Diffraction peaks were measured at room temperature in the *HKL*, $H\bar{K}l$, $\bar{H}KL$, and $\bar{H}\bar{K}L$ octants within the range $2° < 2\theta < 50°$ for a cell ~6.83 × 14.88 × 3.74 Å with the aid of an automated, four-circle diffractometer and monochromatic Mo Kα radiation. Three standards lying approximately out the three reciprocal axes showed

(1) Operated for the U.S. Department of Energy by Iowa State University under Contract No. W-7405-Eng-82. This research was supported by the Office of Basic Energy Sciences, Material Sciences Division.
(2) Corbett, J. D.; Daake, R. L.; Poeppelmeier, K. R.; Guthrie, D. H. *J. Am. Chem. Soc.* **1978**, *100*, 652.
(3) Guthrie, D. H.; Corbett, J. D., submitted for publication in *Inorg. Chem.*
(4) Imoto, H.; Corbett, J. D.; Cisar, A. *Inorg. Chem.* **1981**, *20*, 145.
(5) Guthrie, D. H.; Corbett, J. D. *J. Solid State Chem.* **1981**, *37*, 256.
(6) Cisar, A.; Corbett, J. D.; Daake, R. L. *Inorg. Chem.* **1979**, *18*, 836.
(7) Adolphson, D. G.; Corbett, J. D. *Inorg. Chem.* **1976**, *15*, 1820.
(8) Daake, R. L.; Corbett, J. D. *Inorg. Chem.* **1977**, *16*, 2029.
(9) Daake, R. L. Ph.D. Thesis, Iowa State University, Ames, IA, 1976.

0020-1669/82/1321-1747$01.25/0

Table I. Positional and Thermal Parameters for β-ZrI_2[a]

atom	y[b]	z	B_{11}[c]	B_{22}	B_{33}	B_{12}
Zr 1	0.8849 (3)	0.5000	1.32 (11)	1.64 (10)	1.23 (9)	−0.07 (9)
Zr 2	0.4922 (3)	0.0066 (2)	1.14 (9)	1.31 (9)	1.34 (9)	−0.05 (9)
I 1	0.2745 (3)	0.3945 (2)	1.25 (7)	1.64 (7)	0.94 (7)	−0.04 (6)
I 2	0.2226 (3)	0.8567 (2)	1.60 (8)	1.25 (8)	1.12 (8)	−0.13 (6)
I 3	0.6161 (3)	0.6510 (2)	1.46 (7)	1.43 (7)	1.04 (7)	0.02 (5)
I 4	0.8824 (3)	0.1135 (2)	1.22 (8)	1.47 (7)	1.13 (7)	0.20 (5)

[a] Space group $Pmn2_1$ (no. 31); a = 3.7442 (5) Å, b = 6.831 (1) Å, c = 14.886 (2) Å, and Z = 4. [b] x = 0. [c] Thermal parameters are of the form $\exp[-0.25(B_{11}h^2a^{*2} + B_{22}k^2b^{*2} + B_{33}l^2c^{*2} + 2B_{12}hka^*b^*)]$. $B_{13} = B_{23} = 0$.

no change with time. The crystal was a strong diffractor, and 1580 of the 1763 reflections checked were observed ($I > 3\sigma_I$ and $F > 3\sigma_F$). An absorption correction was applied by using a ϕ-scan method[10] (0–360° in 10° steps at θ = 22.3°, μ = 189 cm^{-1}, 0.816 < T < 0.990). Other programs employed have been referenced earlier.[4]

A likely trial structure considering the lattice dimensions was that of WTe_2, space group $Pmn2_1$ (No. 31). This orthorhombic layered structure is known to be similar to that of β-$MoTe_2$[11] (α-ZrI_2) and has the same relative orientation when the latter's space group $P2_1/m$ is taken with the a axis unique. However, the correctness of the $Pmn2_1$ space group for β-ZrI_2 was not completely certain. Least-squares refinement of the diffraction angles for 15 peaks in the range 41° < 2θ < 47° which were each tuned on both Friedel components gave a = 3.7442 (5), b = 6.831 (1), and c = 14.886 (2) Å when constrained to orthorhombic symmetry (V = 380.7 (1) Å^3, D_x = 6.02 g cm^{-3}). Refinement without restraints gave a = 3.7434 (5) Å, the same values for the other two axes, and angles all within 0.04° (2σ) of 90°. More significant was the fact that a fair number of forbidden reflections ($h0l$, $h + l \neq 2n$) were seemingly observed. Thirteen violations were found every time (two or four measurements) without invoking Friedel's law (the space group is acentric and anomalous scattering was included). These were led by 201 (F_o = 19.0), 407 (15.4), 00$\bar{9}$ (14.3), 007 (14.1), 009 (12.6), and 100 (12.3) in a data set in which 6.2 < F_o < 503.

Accordingly, the structure was initially refined not only in $Pmn2_1$ but in Pm (a axis unique) and $P1$, the only other alternatives. The data were averaged to 768 unique reflections (13 rejected by $|\bar{F}_o - \bar{F}_i| > 8\sigma_F$) in the higher symmetry group and 1487 in the other two. The initial atom positions were those given by Brown[11] for WTe_2. This procedure rapidly resolved the question in favor of the higher symmetry group for which the variation of the positional and isotropic thermal parameters readily yielded R = 0.059 and R_w = 0.119[12] in $Pmn2_1$ vs. 0.077 and 0.128, respectively, for the other two and with distinctly higher uncertainties ($w = \sigma_F^{-2}$). Any real deviations of the structure from the higher symmetry are evidently not sufficient to allow refinement and are not apparent in the final result. Diffuse scattering may be responsible (see later). Elimination of the forbidden reflections from the data set, conversion to anisotropic thermal parameters, and a reweight of 15 groups of reflections sorted on F_o to allow for sixfold dependence of $|F_o - F_c|^2$ in these gave a well-converged result at R = 0.052 and R_w = 0.071. Inversion of the coordinates produced the probably correct configuration as the residuals dropped to 0.051 and 0.070, respectively, without refinement. Inspection of F_o vs. F_c values for ~40 reflections for which the inversion produced the larger changes in F_c supported this conclusion.

A difference map calculated at this point was flat at the atom positions to ±1.5% of the peak height observed in an electron density map. Small components corresponding to layers which had been displaced parallel to b could be readily identified. Integration of these together with the iodine atoms on the electron density map indicated 3.3 and 2.4% populations with displacements of ±0.38 and ±0.16 b relative to the layers in the principal structure. These were not included in any refinement. These components can be identified as shear defects arising from small amounts of the inverted configuration. More puzzling and significant was a large area of residual density (~0.9 × 5.5 × 2.8 Å) in the difference map in the layer x = $^1/_4$, that is, midway between the planes containing all of the atoms. The major axis of this residual corresponded approximately to a projection of metal positions in the chains. No other (iodine) components were present. The maximum peak height corresponded to 1.4% of that of Zr while the integrated area yielded 0.19 Zr. An additional atom reproducibly refined to a 0.042 (6) occupancy with coordinates 0.318 (7), 0.515 (4), and 0.268 (16), and B = 3 (1) Å^2 to yield R = 0.050 and R_w = 0.067, though this accounts for only ~20% of the residual density. The effect of the seventh atom is not included in the distances and structure factors reported later since this does not account for all of the density and its interpretation is ambiguous. The corre-

Table II. Important Distances (Å) in the Independent Units in β-ZrI_2

	Zr–I		
Zr1–Zr2[a]	3.185 (3) × 2	Zr1–Zr2[c]	4.650 (3) × 2
Zr1–Zr1[b]	3.7442 (5) × 2		
Zr1–I1[d]	3.091 (3)	Zr2[a]–I4[a]	3.103 (3)
Zr1–I3	2.901 (4)	Zr2[a]–I2[e]	2.894 (4)
Zr1–I4[c]	2.980 (3) × 2	Zr2[a]–I1	2.972 (3)
Zr1–I2[e]	2.932 (3) × 2	Zr2[a]–I3	2.943 (3)
	Intrasheet I–I		
I1[d]–I2[e]	3.918 (3) × 2	I3–I4[a]	3.926 (2)
I3–I4[c]	2.944 (2) × 2	I1–I2[e]	3.953 (3)
I2[e]–I2[f]	3.7442 (5) × 2	I3–I3[b]	3.7442 (5)
I4[c]–I4[g]	3.7442 (5) × 2	I1–I1[b]	3.7442 (5)
I1[d]–I4[c]	3.908 (2) × 2	I1–I4[a]	3.908 (2)
I2[e]–I4[c]	4.473 (2) × 2	I1–I3	4.474 (3)
I2[e]–I3	4.889 (3) × 2	I2[e]–I3	4.889 (3)
I1[d]–I3	5.899 (3)	I2[e]–I4[a]	5.909 (3)
	Intersheet I–I		
I3–I1[a]	4.148 (2) × 2	I2–I4[a]	4.139 (3) × 2
I2–I3	4.075 (3)	I2–I3[h]	5.152 (3)
I1[a]–I4[a]	5.895 (3) × 2	I1[a]–I4[c]	4.968 (3)

[a] $x + ^1/_2, 1 - y, z - ^1/_2$. [b] $x - 1, y, z$. [c] $x + ^1/_2, -y, z - ^1/_2$. [d] $x, y - 1, z$. [e] $x + ^1/_2, 1 - y, z + ^1/_2$. [f] $x + ^3/_2, 1 - y, z + ^1/_2$. [g] $x + ^3/_2, -y, z - ^1/_2$. [h] $x, y + 1, z$.

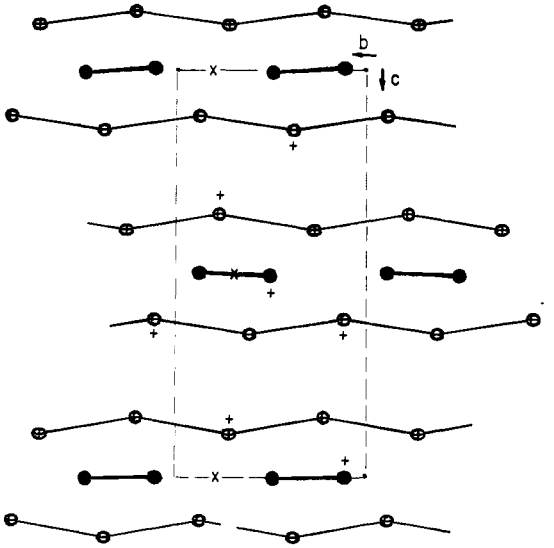

Figure 1. Projection of the structure of β-ZrI_2 along the short a axis, with the zigzag chains of zirconium atoms darkened. All atoms lie on mirror planes at x = 0 and $^1/_2$. The small x's mark pseudocenters of symmetry. Thermal ellipsoids are at the 50% probability level.

(10) Karcher, B. A.; Jacobson, R. A., unpublished program, 1980.
(11) Brown, B. E. *Acta Crystallogr.* **1966**, *20*, 268.
(12) $R = \Sigma||F_o| - |F_c||/\Sigma|F_o|$. $R_w = [\Sigma w(|F_o| - |F_c|)^2/\Sigma wF_o^2]^{1/2}$.

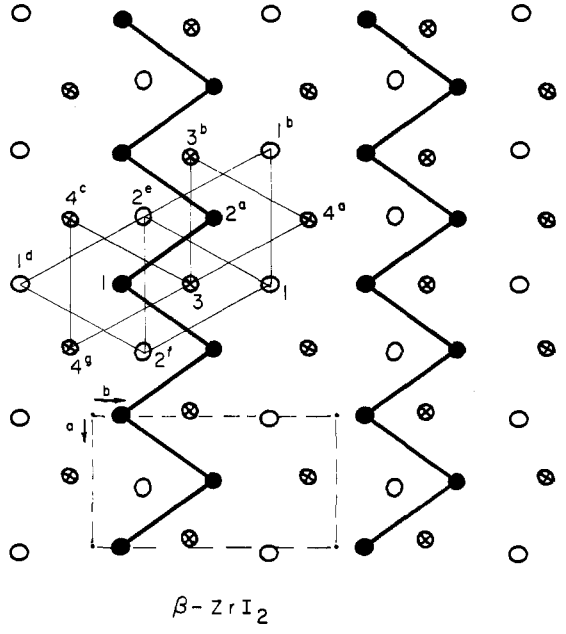

Figure 2. Projection of one sheet of β-ZrI_2 along the *c* axis. The open iodine ellipsoids lie toward the reader with solid zirconium between the iodine layers. The atom identification scheme is given in Table II.

sponding map for α-ZrI_2 indicates some layer displacements but no appreciable extra density.

Results and Discussion

The final positional parameters for β-ZrI_2 are listed in Table I with important distances in Table II. Projections of the structure along the *a* and *c* axes are shown in Figures 1 and 2, respectively, to illustrate the stacking of the layers and the layer structure. For easier comparison, the distances and the views are in the same arrangement as published for α-ZrI_2.[5] The observed and calculated structure factors are available as supplementary material.

The β-ZrI_2 structure does not differ in substance from the prototype determined from film data for WTe_2 by Brown.[11] The iodide is relatively expanded in the sheet dimensions, perhaps because of the greater polarity of this compound, and a number of changes in *y* coordinates correspond to shifts of ≥0.2 Å. The coupling of *z* parameters noted by Brown was not evident. Correlation coefficients of 0.4–0.6 between *y* parameters, some of which are related by pseudoinversion elements, did not interfere.

Both α- ($P2_1/m$) and β- ($Pmn2_1$) ZrI_2 exhibit basically the same structure in which zigzag chains of zirconium atoms lie between essentially double hexagonal close-packed layers of iodine. The former contains two independent but virtually identical chains with one dependent formula unit in each chain while the one type of chain in β-ZrI_2 is generated by two independent ZrI_2 units. The lattice dimensions are closely comparable when α-ZrI_2 is taken with *a* unique, a = 3.741 (α) vs. 3.744 (β) Å, b = 6.821 vs. 6.831 Å, and c = 14.937 vs. 14.886 Å ($c \sin \beta$ = 14.864 Å for the former). The great similarity between α and β extends to distances as well. Only in one case do equivalent separations within the sheets differ by 0.012 Å (3σ) while interlayer separations are all slightly larger in the β-phase, the largest differences being 0.012 Å (4.2σ) and 0.021 Å (4.7σ) The cell volume of β is correspondingly larger by 1.4 (2) $Å^3$, suggesting this phase may be more stable at high temperatures.

The remarkable similarity and interrelationships between these two structures is best appreciated by the superposition of the (100) projections in an ORTEP-generated drawing (Figure 3). This was produced by superimposing only the *b* axes and

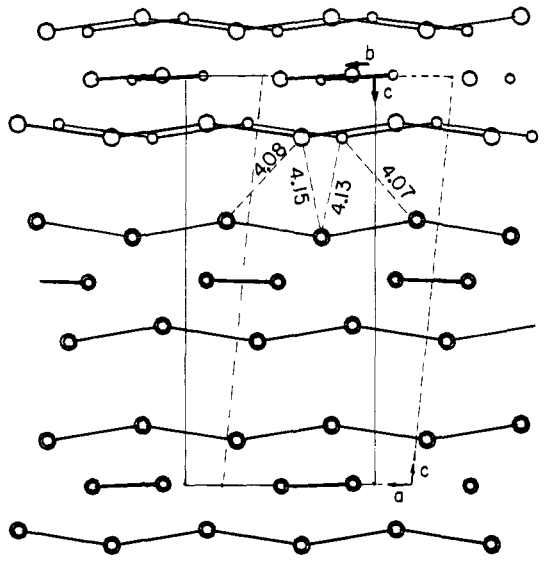

Figure 3. [100] projections of β-ZrI_2 (larger circles and solid cell boundaries) and α-ZrI_2 (*a* axis unique). The *b* axes and the center of the metal chain in the bottom layer in the two structures were superimposed.

the center of the chain projection lying near z = 0. Conversion of β to either α or a possible common supergroup parent is accomplished by alignment of the pseudoinversion centers, three of which are marked with an *x* in Figure 1, along the *c* axis. The latter possibility will be considered later.

The α- and β-ZrI_2 structures nicely represent an alternate means for generating short metal–metal bonds in the presence of significantly larger anions. A number of phases with strong metal–metal bonding in chains and sheets contain parallel chloride or bromide arrays with the same period, a requirement which would be expected to seriously limit the metal-bonding abilities of iodides.[13] In ZrI_2 single zigzag chains which do not run parallel to nonmetal contacts together with appreciable displacement of metal atoms from the center of octahedral interstices exhibit Zr–Zr distances which are 85% of the shortest iodine–iodine distances. Attainment of more extended metal–metal interactions in still lower iodides would appear difficult unless iodine is a distinctly minor component.

Intergrowth. The elucidation of the present structure clears up several problems which have plagued our studies of the diiodide system. Weissenberg photographs of "α" crystals taken after the structure investigation had been accepted for publication revealed a considerably more complex pattern than expected. In the simplest case, additional spots occurred on all festoons with fixed *k* in the 0*kl* photographs but none appeared along 00*l* or elsewhere. These occurred with a fixed displacement for each value of *k*, at somewhat more than $^1/_5$ the normal separation on 01*l*, $^2/_5$ on 02*l*, $^3/_5$ on 03*l*, etc. This feature could not be accounted for by a simple twinning, and a superlattice seemed implausible once it was discovered that the relative intensities of the extra spots varied from crystal to crystal. But an orthorhombic phase with dimensions similar to those of β-ZrI_2 was found to account for these observations when intergrown parallel to [001], that is, along the sheets which are common to both structures (Figure 3). This is easily seen by superposition of the 0*kl* reciprocal nets with common a^* and c^*. The known lattice constants predict an interval of 0.22*k* for the extra spots in 0*kl*. Similarly, Weissenberg photographs for β-ZrI_2 also show extra spots in 0*kl* festoons from intergrown α, and the *h*5*l* reflections are frequently found to have F_o greater than F_c because of accidental overlap. Thus the structures of the terminal members have in fact been

(13) Corbett, J. D. *Acc. Chem. Res.* **1981**, *14*, 245.

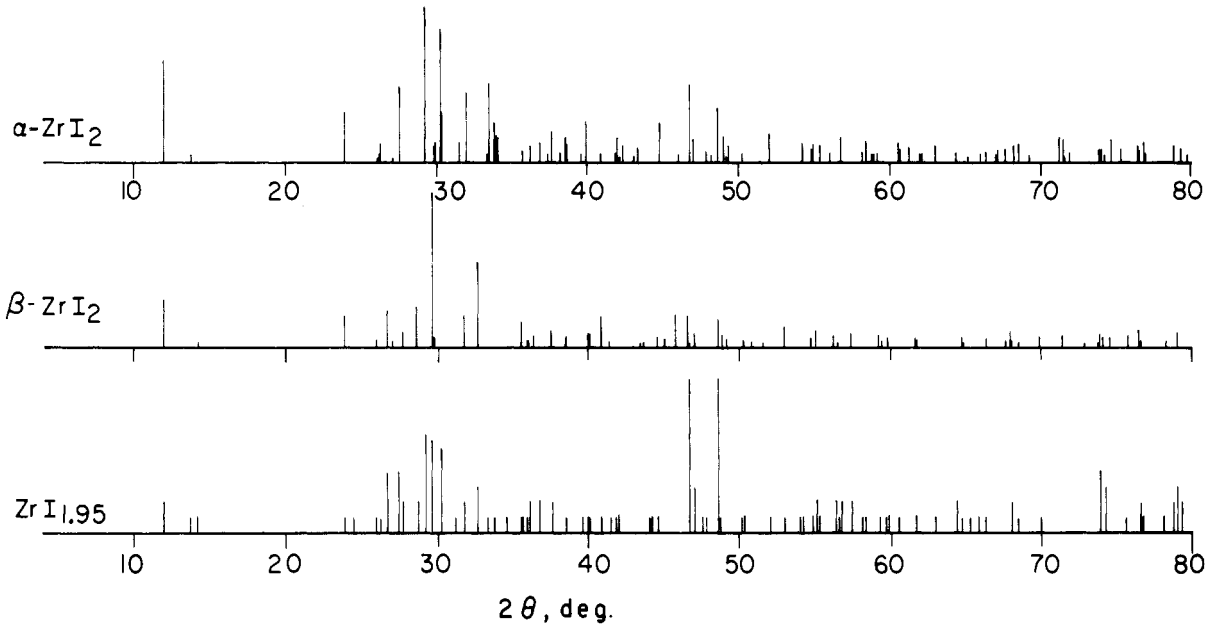

Figure 4. Calculated powder patterns of α-ZrI_2[5] and β-ZrI_2 and the observed Guinier pattern for a sample $ZrI_{1.95\,(5)}$.[9] Preferred orientation is known to affect intensities in the observed pattern.

determined for the major component (~80%) of an intergrown crystal of α- plus β-ZrI_2.

A recent paper by Lopis et al.[14] briefly notes the existence of a series of orthorhombic polytypes of ZrI_2 with $a = 3.74$, $b = 6.93$, and $c = n(14.85)$ Å, where the $n = 24$ polytype had been studied the most. We have seen no evidence for such a superlattice. Were their observations to originate from the described intergrowth, a value of $n = 12$ would appear sufficient to explain the simplest arrangement of extra spots we observe in terms of a superlattice.

Powder Patterns. The complicated powder patterns observed earlier for ZrI_2 can now be understood. Guinier powder patterns obtained from microcrystals of "α-ZrI_2" (which appears to be the major component under many conditions) or from single crystals which had been separated and ground were always considerably more complicated than calculated[15] for the known structure. (The grinding does not appear to be a component of the problem.) It is now clear that this complication arises simply from the presence of varying amounts of β intergrown with α in what appeared to be a reproducible single-phase material. Figure 4 compares a pattern obtained some time ago for a $ZrI_{1.95}$ composition[9] with those calculated separately for α- and β-ZrI_2 components now known. Within the limits imposed by the method the agreement is excellent for a mixture of about 60% α-ZrI_2 and 40% β-ZrI_2. The Guinier method is well-known for its precision in 2θ determination, and the correspondence found is excellent save for five weak, extra lines. On the other hand, the crystals are thin and preferred orientation is a problem since the ground sample is held between sheets of cellophane tape. Such an effect was clearly established for nearly all of the stronger reflections ($I \geq {}^3/_{10}$ by a second pattern obtained from small flakes purposely mounted flat on the tape. Becuase of such uncertainties the intensities shown were estimated only on integral 1–10 scale.

Nonstoichiometry. Some implications regarding a substoichiometry of the intergrown ZrI_2 "phase", but not a solution to the problem, may be found in the diffraction date for β-ZrI_2. Three polycrystalline samples prepared earlier at 700–800 °C in the presence of excess zirconium gave analytical results for I:Zr averaging 1.88:1 with weight recoveries of Zr plus I of 100 ± 0.11%.[9] The probable error in the ratio is though to be ~0.05. Nonetheless, the structure results for both the α and β phases contain no evidence for any interstitial atoms such as occur between the layers in the ordered superstructures for several $Zr_{1+x}Cl_2$ phases.[6]

The possibility of a significant nonstoichiometry in the intergrowth (or other defect) regions still remains, though direct evidence regarding this is much more difficult to acquire. Presumably the intergrowth boundary contains an appreciable region of local disorder, principally because of the difference in the angles of the c axes to the layers. Although the diffraction spots from the two phases are usually quite sharp, the amount of diffuse scattering in low-angle streaks parallel to b^* in the $0kl$ Weissenberg photographs varies from negligible to heavy for both phases and even from crystal to crystal in the same preparation. The β-ZrI_2 data crystal exhibited a moderate streak. Some crystals exhibit enough structure to this streak that two or three additional, diffuse festoons can be defined at low angles, corresponding to a doubling of b. A defect in or about neighboring chains which would cause this is not obvious with present information.

The final difference map for β-ZrI_2 (see Experimental Section) contained two interesting features. First was evidence for small amounts (2–3%) of systematic stacking defects in the form of lateral layer displacements, apparently from a small twin component. More pertinent to the question of nonstoichiometry was the occurrence of an area of extra but diffuse electron density along the projection of the chains and lying midway between the planes $x = 0, {}^1/_2$ which contain all of the atoms in the normal structure. However, no extra peaks corresponding to iodide partners occur in this section and the extra density is probably too close to Zr in a defect-free array. This leaves one stuck with the premise that extra, evidently interstitial, zirconium may be present which scatters coherently with the major part of the crystal which the iodine host does not. On the other hand it may also arise solely from the defects which give rise to the diffuse streaking and spots just described.

A zirconium atom at 0.042 (6) occupancy may be refined in this region, making the overall composition $Zr_{1.92\,(1)}I_2$.

(14) Lopis, Kh. S.; Troyanov, S. I.; Tsirel'nikov, V. I. *Russ. J. Inorg. Chem. (Engl. Transl.)* **1979**, *24*, 1306.
(15) Clark, C. M.; Smith, D. K.; Johnson, G. J. "A Fortran IV Program for Calculating X-ray Powder Diffraction Patterns-Version V"; Department of Geosciences, The Pennsylvania State University: University Park, PA, 1973.

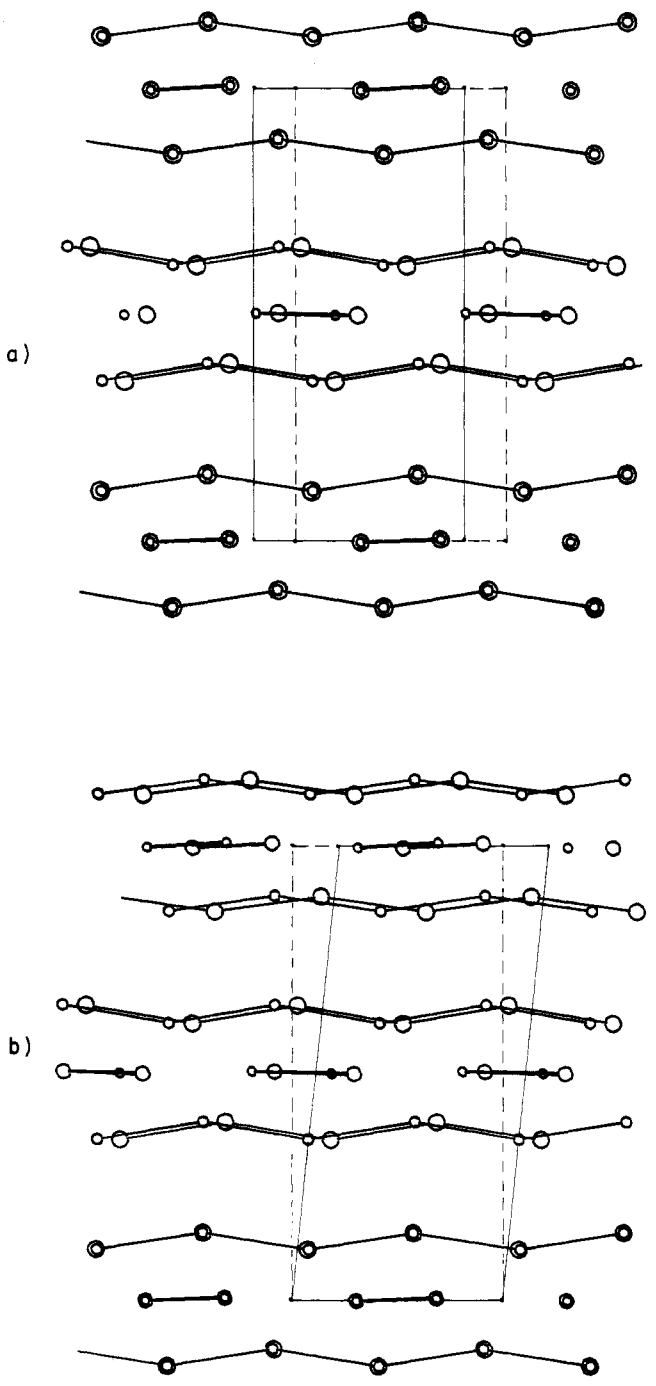

Figure 5. Superposition of the [100] projections of each of the ZrI_2 structures (larger spheres and solid cell outline) with that of their supergroup parent (*Pmnb*, small spheres and dashed outline): (a) β-ZrI_2 ($Pmn2_1$); (b) α-ZrI_2 ($P2_1/m$, *a* axis unique).

However, this atom is too close to others to be a plausible component of the ordered structure, and it does not account for all the apparent extra electron density. Thus the structural data do not contain a very satisfying solution to the substoichiometry question.

A Common Supergroup. The similarities in structure and cell dimensions of α- and β-ZrI_2 as well as their intergrowth property suggest that both may represent subgroups of a higher symmetry precursor which might exist at high temperature. The disposition of the second and third sheets in the two structures, especially with regard to the shortest interlayer distances marked in Figure 3, immediately suggests this parent occurs at the midpoint in the relative layer displacements. The addition of an inversion center to $Pmn2_1$ or an *n* glide to $P2_1/m$ directly provides the appropriate supergroup of both in the lattice (translation) equivalent $P2_1/m\ 2_1/n\ 2_1/\beta = Pmnb$, a nonstandard setting of No. 62.

The shear displacements necessary to convert the hypothetical supergroup (*s*-ZrI_2) phase to the two maximal subgroups are illustrated in Figure 5. Starting with a fixed bottom layer, the polar β-ZrI_2 is obtained by shear displacements of successive sheets by a small amount in opposite directions (top), where the displacements necessary to generate α-ZrI_2 are equal but all in the same direction (bottom). The conversion of *s*-ZrI_2 (D_{2h}) to either α-ZrI_2 (C_{2h}) or β-ZrI_2 (C_{2v}) meets the criteria for a second- (or higher) order phase transition. A summit position of *s*-ZrI_2 with respect to interlayer contacts (Figures 3 and 5) would be expected to require some expansion along *c* and thereby favor its formation only at higher temperatures. Further conversion of *s*-ZrI_2 to 4H-CdI_2 through elimination of the metal displacements which allow Zr–Zr bonding is symmetry allowed but probably not very likely in view of the properties of ZrI_2.

Whether α- or β-ZrI_2 is the more stable when formed and whether the hypothetical *s*-ZrI_2 actually exists are hard to determine with present information. The very great dimensional similarities of α and β suggest the enthalpy change for their conversion must be very small, and so perhaps only a slightly greater molar volume might favor β-ZrI_2 at higher temperatures. The observed character of the intergrowth implies that kinetic (nucleation) factors are more important than actual stability under the usual synthetic conditions (600–775 °C) and during subsequent cooling to room temperature. The best crystals of α and β studied each had the other as a minor component in only one orientation, as described earlier, although crystals with additional intergrowth components, usually in the complementary orientation, were often found. Transformation of *s*-ZrI_2 on cooling does not appear to have occurred since extensive twinning was not found in most of the crystals studied. The transition to *s*-ZrI_2 is therefore presumed to lie above the usual temperatures employed for synthesis. Indeed, visibly twinned crystals and two orthorhombic crystals for which the structure would not refine well, presumably because of disorder (see Experimental Section), came from synthesis reactions at 900 and 950 °C.

Although a continuous, first-order transition analogous to α- → β-ZrI_2 has been observed on cooling $MoTe_2$ to ~250 K,[16] this change evidently does not occur at all readily with the iodide. Rather (α,β)-ZrI_2 is very slowly converted to a third polymorph, Zr_6I_{12}, above 800 °C, but perhaps only via a vapor-phase transport process.[3]

Acknowledgment. The authors are particularly indebted to Professors H. F. Franzen and R. A. Jacobson for helpful discussions regarding phase transitions and crystallography, respectively.

Registry No. β-ZrI_2, 15513-85-6.

Supplementary Material Available: A listing of structure factor amplitudes (2 pages). Ordering information is given on any current masthead page.

(16) Clarke, R.; Marseglia, E.; Hughes, H. P. *Philos. Mag.* [*Part*] *B* **1978**, *38*, 121.